

2.3 Fatigue test procedure

Fatigue tests were carried out in air at room temperature using a servo-hydraulic combined axial/torsional fatigue testing machine. The nominal shear stress amplitude in cyclic torsion was $\tau_a = 1000$ MPa (the true shear stress amplitude was $K_t \tau_a = 1060$ MPa). A nominal static compressive axial stress of $\sigma_s = -1200$ MPa (the true static compressive axial stress was $K_t \sigma_s = -1390$ MPa) was simultaneously applied to suppress a possible Mode I fatigue crack growth that causes kinking and branching. The test frequency, f , was either 0.1 Hz or 10 Hz. The stress ratio of cyclic shear stress was $R = -1$. Measurement of surface crack length was made by the replica method by halting the testing machine at every scheduled number of cycles.

3. EXPERIMENTAL RESULTS

Just after fatigue testing, the hydrogen content in the notched region of a specimen was measured with TDA up to 300 °C. Consequently, H-charging specimens tested at $f = 0.1$ Hz and $f = 10$ Hz contained hydrogen of 0.40 and 0.47 mass ppm, respectively.

In the previous study (Akaki 2017), the fatigue test was carried out with non-charging and H-charging specimens at a test frequency of $f = 2$ Hz under the same mechanical conditions of $\tau_a = 1000$ MPa, $\sigma_s = -1200$ MPa and $R = -1$. From this result, it was found that both Mode I and shear-mode (Mode II on the surface) fatigue crack growth behaviours were greatly affected by hydrogen and thereby their rates were accelerated. In the present study, to investigate the effect of frequency in a hydrogen environment, fatigue tests of shear-mode cracks were carried out using H-

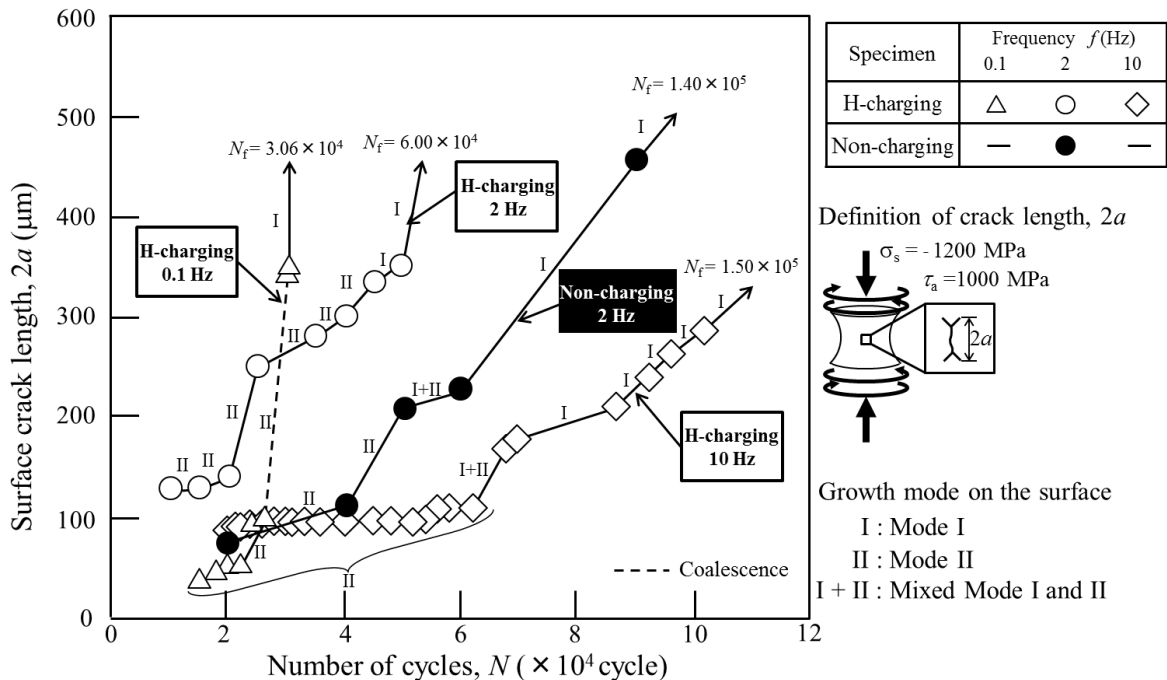


Fig. 4 Effect of frequency on Mode II crack growth behavior in H-charging and non-charging specimens subjected to $\tau_a = 1000$ MPa, $\sigma_s = -1200$ MP at $R = -1$.

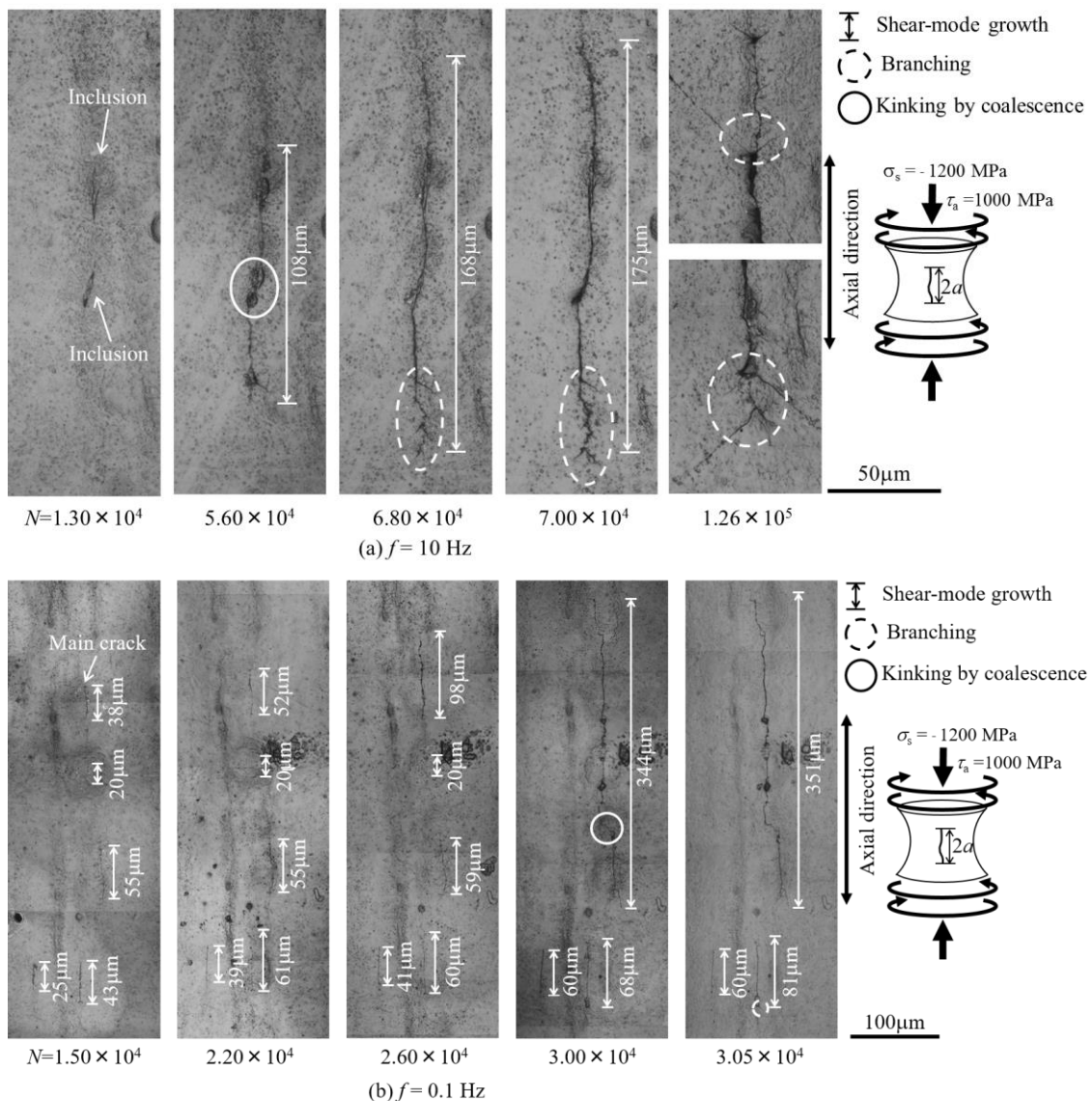


Fig. 5 Mode II crack growth behavior in H-charging specimens subjected to $\tau_a = 1000 \text{ MPa}$ and $\sigma_s = -1200 \text{ MPa}$ at $R = -1$ and different frequencies of (a) $f = 10 \text{ Hz}$ and (b) $f = 0.1 \text{ Hz}$ (replica method).

charging specimens at two cyclic frequencies of $f = 0.1 \text{ Hz}$ and 10 Hz in addition to previous $f = 2 \text{ Hz}$ (Akaki 2017) under the same mechanical condition.

Fig. 4 represents the relationship between fatigue crack length and number of cycles for the H-charging and non-charging specimens tested under the same mechanical conditions of $\tau_a = 1000 \text{ MPa}$, $\sigma_s = -1200 \text{ MP}$ and $R = -1$ but for different frequencies, f , of 0.1 Hz , 2 Hz and 10 Hz . In this figure, I, II and I+II indicate Mode I, Mode II and mixed Mode I and II fatigue crack growths observed on the surface of specimen, respectively. As shown in **Fig. 4**, the crack length, $2a$, was defined by the length measured in the axial direction regardless of irregular crack path. From this figure, it is found that:

- (1) Hydrogen environment accelerated the crack growth rate.

- (2) H-charging specimen tested at $f = 2$ Hz and 0.1 Hz fractured by load cycling of approximately 1/4 or smaller number of cycles, N_f , compared to $f = 10$ Hz.
- (3) N_f for H-charging specimen tested at $f = 10$ Hz was comparable to that for non-charging specimen tested at $f = 2$ Hz.

Fig. 5 shows that the crack growth behavior at $f = 0.1$ Hz and 10 Hz observed in H-charging specimens by the replica method. For H-charging specimen tested at $f = 10$ Hz, the cracks that initiated from two collinear inclusions propagated in the axial direction and coalesced with each other. Subsequently, the crack continued to propagate in the form of shear-mode crack repeating small branching. Finally, the crack caused a large branching and steadily continued Mode I propagation in the approximately 45° direction with respect to the axial direction, leading to specimen fracture. The number of cycles to failure was 1.50×10^5 cycles. In contrast, for H-charging specimen tested at a low frequency of $f = 0.1$ Hz, the number of cycles to failure was 3.06×10^4 cycles, i.e., about 1/5 smaller than at $f = 10$ Hz. A visible inclusion was not present at the crack initiation site but alternatively, a number of parallel cracks initiated closely in a specific area on the smooth surface. These multiple shear-mode cracks coalesced with each other and grew into a major shear-mode crack. The nearly pure shear-mode fatigue crack growth was confirmed at least until 3.05×10^4 cycles. Thereafter, the crack was branched and the specimen fractured immediately by a fatigue loading of only 80 cycles. At this low frequency, Mode I crack growth rate was thus markedly accelerated after branching in a hydrogen environment, despite the heavy compressive stress acting on the crack surface.

4. DISCUSSION

The average growth rate of shear-mode cracks, $(da/dN)_{II, ave}$, from the crack initiation to complete Mode I branching was calculated to be $(da/dN)_{II, ave} = 1.24 \times 10^{-9}$ m/cycle for H-charging specimen tested at $f = 10$ Hz, while for $f = 0.1$ Hz, it was $(da/dN)_{II, ave} = 1.01 \times 10^{-8}$ m/cycle, which was approximately 8 times greater than for $f = 10$ Hz, i.e., the effect of hydrogen became pronounced with decreasing frequency. In addition, Figs. 5(a) and 5(b) show the whole processes of fatigue crack growth behaviors in H-charging specimens at $f = 10$ Hz and 0.1 Hz, respectively, which were observed by the replica method. In Fig. 5(a) for $f = 10$ Hz, a shear-mode crack propagated almost solely and after it reached a length, $2a$, of 108 μ m, many branched cracks were intermittently generated forming a multiple forked crack. This may be because a mechanical condition of branching was satisfied although the static compressive stress ($\sigma_s = -1200$ MPa) worked to suppress the continuous growth of Mode I branched cracks. When the crack length, $2a$, reached 181 μ m, a continuous Mode I crack growth started but the acceleration of its growth rate is still low due to the heavy compressive stress component acting on the crack surface of a Mode I crack. This is similar to the results that were previously obtained for non-charging specimen tested at $f = 2$ Hz (Akaki 2017) as well as the other result obtained in the absence of hydrogen (Matsumaga 2010, Endo 2015). On the other hand, at a low frequency of $f = 0.1$ Hz, as seen in Fig. 5(b), a number of in-line shear-mode cracks initiated simultaneously, then they propagated at comparatively high growth rate as a shear-mode crack and finally grew into a long shear-mode crack by their coalescence. The length of shear-mode crack ($2a$

= 351 m) was longer than that for $f = 10$ Hz ($2a = 181$ m). In addition, the multiple forked crack that was observed at $f = 10$ Hz was not observed at $f = 0.1$ Hz. After Mode I branching, the specimen fractured immediately by load cycling of only 80 cycles. The difference in those crack growth behaviors is thus responsible for a significant difference in fatigue life, N_f , between $f = 0.1$ Hz and $f = 10$ Hz. Yamabe (2012) conducted a Mode I fatigue crack growth test for a bearing steel of JIS-SUJ2 at different frequencies of $f = 0.2$ Hz, 2 Hz and 20 Hz. They reported that Mode I fatigue crack growth rate of hydrogen-charged specimens was strongly dependent on the cyclic frequency. They found that the secondary cracks ahead of a primary crack initiated by the influence of hydrogen and the fatigue crack growth rate was accelerated by their coalescing with the primary crack. In the present study of shear-mode fatigue crack growth, a secondary crack was not observed. However, because of both the coalescence of many coaxial cracks and the rapid shear-mode fatigue crack growth, the growth rate was significantly enhanced for a low frequency of 0.1 Hz. As a result, the shear-mode fatigue crack growth behavior had a similar tendency as Mode I fatigue crack growth behavior, i.e., the effect of hydrogen became greater for low frequency. This is commonly interpreted to be because more hydrogen can diffuse and concentrate at crack tip in a cycle at low frequency.

Both for $f = 10$ Hz and $f = 0.1$ Hz, debris generated along the crack. Debris was in red-brown and thus it is considered to be an oxide powder caused by cyclic reciprocating sliding contact of crack surfaces. A larger amount of debris was observed for $f = 10$ Hz than for $f = 0.1$ Hz. Further, as seen in Fig. 5, the crack is thicker for $f = 10$ Hz than for $f = 0.1$ Hz. These results imply that the crack face interference could be greater for $f = 10$ Hz than for $f = 0.1$ Hz. Therefore, in the shear-mode crack growth, not only the slip localization is enhanced, but the sliding-mode crack closure may be inhibited by hydrogen. (Tscheegg 1983, Tscheegg 1983, Ritchie 1985).

5. CONCLUSIONS

The effect of cyclic frequency on the shear-mode fatigue crack growth behavior of a bearing steel of JIS-SUJ2 in a hydrogen environment was investigated. The frequency ranged from 0.1 to 10 Hz. The following results were obtained:

- (1) The growth rate of a shear-mode fatigue crack was significantly increased with decreasing frequency, i.e., the shear-mode fatigue crack exhibited a strong dependency of growth rate on frequency as well as a Mode I fatigue crack.
- (2) At low cyclic frequency, a number of small cracks initiated simultaneously in a specified region on the specimen surface and shortly they coalesced each other forming a shear-mode crack. The growth rate for both the shear-mode crack and the subsequent Mode I branched crack was very high, leading to rapid failure.
- (3) The shear-mode fatigue crack produced more debris and thereby it was thicker for high frequency than for low frequency. Therefore, the crack growth rate is considered to be influenced by sliding-mode crack closure in addition to the localization of slip deformation.

REFERENCES

M.-H. Evans. (2012), "White structure flaking (WSF) in wind turbine gearbox bearings:

- effects of 'butterflies' and white etching cracks (WECs)", *Mater. Sci. Technol.*, **7**(2), 3-22.
- M.-H. Evans, A.D. Richardson, L. Wang and R.J.K. Wood. (2013), "Serial sectioning investigation of butterfly and white etching crack (WEC) formation in wind turbine gearbox bearings", *Wear*, **302**(1-2), 1573-1582.
- Tanimoto H, Tanaka H and Sugimura J. (2011), "Observation of Hydrogen Permeation into Fresh Bearing Steel Surface by Thermal Desorption Spectroscopy" *JSME. A.*, **6**(7), 291-296.
- Kino N and Otani K. (2003), "The influence of hydrogen on rolling contact fatigue life and its improvement", *JSE Review*, **24**(3), 289-294.
- Tamada K and Tanaka H. (1996), "Occurrence of brittle flaking on bearings used for automotive electrical instruments and auxiliary devices", *Wear*, **199**(12), 245-252.
- Fujita S, Matsuoka S, Murakami Y and Marquis G. (2010), "Effect of hydrogen on Mode II fatigue crack behavior of tempered bearing steel and microstructural changes", *Inter. J. F.*, **32**(6), 943-951.
- Murakami Y, Kanazaki T, Mine Y and Matsuoka S. (2008), "Hydrogen embrittlement mechanism in fatigue of austenitic stainless steels", *MMS and ASM Inter.*, **39**(6), 1327-1339.
- Tanaka H, Homma N, Matsuoka S and Murakami Y. (2007), "Effect of Hydrogen and Frequency on Fatigue Behavior of SCM435 Steel for Storage Cylinder of Hydrogen Station", *JSME. A.*, **73**(736), 1358-1365.
- Matsuoka S, Tsutsumi N, and Murakami Y. (2008) "Effects of Hydrogen on Fatigue Crack Growth and Stretch Zone of 0.08 mass%C Low Carbon Steel Pipe", *JSME. A.*, **74**(748), 44-53.
- Murakami Y, Matsuoka S, Kondo Y and Nishimura S. (2012), "Mechanism of Hydrogen Embrittlement and Guide for Fatigue Design", Hongo 5 Chome 30-15, Bunkyo-ku, Tokyo, JAPAN 113-0033 *Yokendo Ltd.*
- Yamabe J, Matsumoto T, Matsuoka S and Murakami Y. (2012), "A new mechanism in hydrogen-enhanced fatigue crack growth behavior of a 1900-MPa-class high-strength steel", *Inter. J. F.*, **177**(2), 141-162.
- Akaki Y, Matsuo T, Nishimura Y, Miyakawa S and Endo, M. (2017), "A new testing method for investigating the shear-mode fatigue crack growth behavior in hydrogen environment", Proceedings of *Damage of Assessment of Structures* to be presented.
- Matsumaga H, Shomura N, Muramoto S and Endo M. (2010), "Shear-mode threshold for a small fatigue crack in a bearing steel", *FFEMS.*, **34**(1), 72-82.
- Endo M, Okazaki S, Matsunaga H, Moriyama S, Munaoka K. and Yanase K. (2015) "A new fatigue testing machine for investigating the behavior of small shear-mode fatigue cracks. *J. Exp. Tech.*, **40**, 1065-1073.
- Tschegg EK. (1983), "Sliding mode crack closure and mode III fatigue crack growth in mild steel", *Acta Metall.*, **31**(9), 1323-1330.
- Tschegg EK. (1983), "A contribution to mode III fatigue crack propagation" *Mater. Sci. Engi.*, **54**(1), 127-136.
- Ritchie RO, McClintock FA, Tschegg EK and Nayeb-Hashemi. (1985), "Mode III fatigue crack growth under combined torsional and axial loading", *ASTM STP.*, **853** 203-227.